NASA CR-145037

EVALUATION OF TWO SWEPT-INFINITE-WING POTENTIAL/VISCOUS-FLOW COMPUTER PROGRAMS

(NASA-CR-145037) EVALUATION OF TWO SWEPT-INFINITE-WING POTENTIAL/VISCOUS-FLOW COMPUTER PROGRAMS (Tennessee Univ.) 23 p HC \$3.50 CSCL 01A
N76-32129
Unclas
G3/02 05323

by

Rao V. Arimilli

NASA-ASEE Summer Faculty Research Fellow
University of Tennessee, Knoxville

National Aeronautics and
Space Administration

August 1976

EVALUATION OF TWO SWEPT-INFINITE-WING POTENTIAL/VISCOUS FLOW COMPUTER PROGRAMS

Rao V. Arimilli*

SUMMARY

Evaluation is made of two computer programs capable of predicting the potential and viscous interacting flow around wings of infinite aspect ratio. The programs are compared in terms of their capabilities, the approximations and the methods of solution used, and the input requirements. Six airfoils, each representative of a class of airfoils, are used as test airfoils. The results predicted by the programs are presented for each airfoil at sweep angles of 0°, 20°, and 40° over a range of angles of attack. The results show that at zero sweep both programs predicted the aerodynamic coefficients well and generally in good agreement with measurements. At 20° and 40° of sweep, as there are no experimental data available, definitive conclusions cannot be drawn about the accuracy of the predictions although the results are presented and discussed. The execution times are approximately the same for the two programs.

INTRODUCTION

The present day aerodynamics designer has a number of computer programs (ref. 1) available as tools for design. While most of these programs are based on potential-flow analysis, a limited number (refs. 2 and 3) are available that solve the potential-viscous interacting flow in two dimensions. However, to date the author knows of only two programs that predict the aerodynamic characteristics of swept-infinite wings. (See refs. 4 and 5.) Swept-infinite wings are swept wings of infinite aspect ratio or infinite span. Although swept-infinite wings do not appear to be directly usable in aerodynamics or hydrodynamics, knowledge of the prediction methods for swept-infinite wings should

*NASA-ASEE Summer Faculty Research Fellow,
University of Tennessee, Knoxville

be useful and perhaps the necessary first step in the ultimate goal of the prediction of the characteristics of finite wings.

The aim of this paper is to compare, from the user's viewpoint, the swept-infinite wing potential/viscous flow programs of Dvorak and Woodward (ref. 4) and Gingrich and Bonner (ref. 5) for single-element wings. Because of the proprietary nature of the latter program, details of it will be discussed only sketchily here. However, six test airfoils are run on both programs, and the results are presented and compared. In the unswept orientation, the two predictions are also compared with those of reference 3 with some in-house modifications made at NASA Langley Research Center (ref. 6).

SYMBOLS

The units used for the physical quantities of this paper are given both in the International System of Units (SI) and in the U.S. Customary Units. The symbols enclosed in parenthesis are used in plotting the results.

C	airfoil normal chord, cm (in.)
C_D(CD)	drag coefficient, $\frac{D}{\frac{1}{2}\rho U_\infty^2 C}$
C_L(CL)	lift coefficient, $\frac{L}{\frac{1}{2}\rho U_\infty^2 C}$
D	drag force per unit span, N (lbf)
L	lift force per unit span, N (lbf)
M_∞	free-stream Mach number
RN	Reynolds number = $U_\infty C/\nu$
U_∞	free-stream velocity, m/sec (ft/sec)

x	coordinate along the normal chord line, cm (ft)
α(ALPHA)	angle of attack (angle between the streamwise chord and the free-stream direction), deg
Λ	sweep angle, deg
ν	kinematic viscosity of air, m^2/sec (ft^2/sec)
ρ	density of air, kg/m^3 ($slugs/ft^3$)

COMPARISON OF PROGRAMS

The two programs are compared in terms of their capabilities, the approximations used, and the methods of solution in the following table:

DVORAK AND WOODWARD PROGRAM (DWP)	GINGRICH AND BONNER PROGRAM (GBP)
1. Program capabilities:	
(a) Has two-dimensional and swept capability.	- Same -
(b) Has multi-element capability up to one slat, one main element and two flaps.	Has capability for a single element sharp trailing-edge airfoil only.
2. Overall method of analyses:	
Analysis is based on potential/viscous interacting flow.	- Same -
3. Type of flow assumed:	
Incompressible flow analysis is used.	Incompressible flow analysis with Labrujere (ref. 7) corrections for compressibility effects is used.
4. Simplifications used in the 3-D flow:	
Independence principle is used.	- Same -
5. Method of potential-flow solution used:	
Pressure distribution is determined perpendicular to the leading edge using a two-dimensional vortex sheet technique with an alternate formulation for blunt trailing edges.	Pressure distribution is determined using the two-dimensional conformal transformation of Theodorsen for incompressible flow.

	DWP	GBP
6.	Coupling between potential and viscous solutions:	
	Boundary-layer displacement effect is introduced into the potential flow by an equivalent source distribution. Thus eliminating the necessity of inverting a new influence coefficient matrix for each inviscid-viscous iteration.	The method of Spence (ref. 8) is used to establish the effect of the displacement surface on the potential flow.
7.	Type of boundary-layer method used:	
	Integral boundary-layer methods are used on all surfaces except the upper surfaces of the flaps.	Integral boundary-layer method are used on both surfaces of the single element.
8.	Determination of program starting conditions:	
	To start computations, integral properties on the stagnation line are determined by the method of Cumpsty and Head (ref. 9).	- Same -
9.	Method of laminar boundary-layer solution:	
	Laminar boundary-layer growth is calculated using a two-dimensional integral method along external streamlines. A check is made for laminar separation, free transition, and forced transition.	For laminar boundary-layer calculations, the approximate three-dimensional integral method of Smith and Young (ref. 10) is used with extensions to adiabatic compressible flow.
10.	Determination of laminar separation:	
	A correlation between the pressure gradient parameter and Reynolds number based on momentum thickness is used to predict laminar separation and possible reattachment as a turbulent boundary layer.	Separation is predicted when shear stress in the normal chord direction becomes zero.
11.	Determination of transition:	
	Transition criteria are based on the streamwise boundary-layer parameters (refs. 11 to 13). Crossflow instability is not considered.	- Basically the same (see refs. 11 and 14) - Crossflow instability analysis of Brown (ref. 15) is extended and used.

DWP	GBP

12. Method of turbulent boundary-layer solution:

DWP	GBP
Turbulent boundary-layer development in the streamwise and the crossflow direction is calculated by the three-dimensional integral method of Cumpsty and Head (ref. 16). The relationship between the streamwise and crossflow profiles suggested by Mager (ref. 17) is also used.	Turbulent boundary layer is treated with the three-dimensional integral method of Smith (ref. 18). Small crossflow assumption is not made.

13. Determination of turbulent separation:

DWP	GBP
Turbulent separation is predicted when the angle between the normal chord and skin-friction direction becomes 90°.	Separation is predicted when shear stress in the normal chord direction becomes zero.

14. Determination of drag coefficient:

DWP	GBP
Drag coefficient is determined from Squire and Young (ref. 19) formula using streamwise boundary-layer parameters at the trailing edge.	Squire and Young formula is extended for small crossflow and used to determine the drag coefficient.

15. Convergence of the potential-viscous solution:

DWP	GBP
During any iteration, if the lift coefficient is within 0.01-0.015 (the actual in-between value to be chosen by the user) of the previous iteration, the solution is considered to converge.	Convergence criterion is that the change in circulation between two successive iterations be less than a certain value. This condition is enforced when the difference between the velocities on the upper and lower surfaces become a small fraction of the free-stream velocity.

INPUT-OUTPUT REQUIREMENTS

The purpose of this section is to compare from the user's viewpoint the two programs in terms of their input and storage requirements. For convenience, the comparisons are tabulated:

	DVORAK AND WOODWARD PROGRAM (DWP)	GINGRICH AND BONNER PROGRAM (GBP)
1.	Airfoil geometry is to be input by the coordinates of upper and lower surfaces, in each case, from the L.E. to the T.E. Intersection of the surface with the reference line must be the L.E. point (first point on each surface). The coordinates should be input dimensionless but not in percentages.	Coordinates of the wing are to be input from the leading edge (L.E.) to the trailing edge (T.E.) on the upper surface and continued from the T.E. to the L.E. on the lower surface in a clockwise direction.
2.	Maximum number of input coordinate points is limited to 30 on each of the surfaces.	Total number of input points around the airfoil is limited to 50.
3.	Flow parameters to be input are the free-stream RN, Mach number and velocity, and the normal chord length. For single-element cases, the program uses only the RN.	Flow parameters to be input are the free-stream Mach number, stagnation temperature and pressure and the normal (not streamwise) chord. Program calculates the RN.
4.	Program interprets the input angle of attack as the angle relative to the input reference chord line.	Program calculates the longest chord-line and the input angle of attack is taken with respect to the longest chord line.

NOTE: In both programs, the input parameters should be based on the geometric parameters in the unswept orientation of the wing.

	DVORAK AND WOODWARD PROGRAM (DWP)	GINGRICH AND BONNER PROGRAM (GBP)
5.	Transition can be free or forced. For forced transition, x/c value at which transition is desired should be input. Both the upper and lower surfaces get tripped at the same x/c location.	Transition can be free or forced. For forced transition, the input coordinate point number that represents the x/c at which transition is desired should be specified.
6.	In the event of separation without reattachment, the output does not clearly state the result. Instead the computations continue without interruption. It appears that the condition for separation without reattachment is not satisfied for any of the six test airfoils.	The program does not model the possibility of reattachment in the event of laminar separation.
7.	Aerodynamic coefficients are based on the chord length normal to the L.E.	Aerodynamic coefficients are based on the streamwise chord length.

DWP	GBP
8. Program required 150K octal words of memory.	It required under 65K octal words of memory.
9. A numerical value for convergence criterion on C_L is required as an input. The user can choose a value between 0.01 and 0.015. The user can also input the maximum number of iterations as an additional parameter.	User has no direct control on convergence criterion. Indirectly, the user may input the maximum number of iterations as a parameter. This number is not to exceed 15.

RESULTS AND DISCUSSION

The following six airfoils, each representative of a class of airfoils, as indicated, were chosen as the test cases: (1) NACA 0012 airfoil, uncambered, 12 percent thick; (2) NACA 2424 airfoil, slightly cambered but with a much higher thickness of 24 percent chord; (3) NACA 63-006 airfoil, symmetric 6-percent-thick airfoil designed for low drag; (4) NACA 23012 airfoil, cambered version of NACA 0012 airfoil; (5) GA(W)-1 airfoil, advanced technology general aviation airfoil designed for wide C_L range without flow separation, 17-percent-thick with substantial camber near the trailing edge, a reflexed lower surface contour, and a blunt trailing edge; and (6) TN-D 7071 airfoil (see ref. 24), designed for maximum lift, maximum thickness 12.5-percent chord, located at approximately 25 percent chord from the leading edge.

For each airfoil, one computer job was run at a fixed sweep angle in order to compute a number of angle-of-attack cases. Three such jobs, one each corresponding to the sweep angles of 0°, 20°, and 40°, were run for each airfoil through the two programs under consideration. For the unswept orientation, the airfoils were also run through the program of reference 3 updated with in-house modifications at Langley (ref. 6).

In the unswept orientation for each of the test-case airfoils, aerodynamic coefficients predicted by the three programs are compared with the experimental results available in the literature. For the infinite-span airfoils in the swept orientation, experimental data for C_L and C_D do not exist in the open literature at the present time. There is some published boundary-layer data for a few swept-wing cases (refs. 20 and 24) primarily for the purpose of evaluating three-dimensional turbulent boundary-layer computational methods. Therefore, conclusions cannot be drawn about agreement between the predictions and measurements for wings in swept orientation.

The airfoil-surface coordinates, chord length, Reynolds number, and the angle of attack input into both programs are based on the unswept orientation or what is called by the authors of both programs as the reference orientation. However, the output aerodynamic coefficients of Dvorak and Woodward are based on the reference (that is,normal) chord; whereas, those of Gingrich and Bonner are based on the streamwise chord. It is, therefore, necessary to point out that all the results presented in this report are based on the streamwise chord.

There is one other point that requires mention here. For all cases,the Gingrich and Bonner Program (GBP) first calculates the longest chord and the input angle of attack is then interpreted to be the angle of attack of the flow with respect to the longest chord. For most airfoils, the reference line (the line with respect to which the airfoil surface coordinates are specified) is coincident with the longest chord line. Of the six test-case airfoils, the TN D-7071 airfoil is the only one with a reference line that is not coincident with the longest chord line. The angle between the two lines for this airfoil is 5.03476°. However, experimental as well as the Dvorak and Woodward results for all airfoils are based on the angle of attack defined with respect to the input reference line. Therefore, for proper comparisons with these results, the angles of attack for the TN D-7071 airfoil are adjusted by adding 5.03476° to the value of the angle of attack listed on the output.

Both programs have the ability to continue computations, without encountering numerical difficulties, for as much as 15° (depending on the airfoil) past the angle of attack at which trailing edge separation has first occurred. In other words, calculatations can be continued beyond the case of the small separation by incrementing the angle of attack until the boundary layer has separated over much of the upper surface even though such predictions cannot be meaningful because the boundary-layer approximations used in the analysis are no longer valid. Therefore, results are presented only for those angle-of-attack cases in which there is no separation at all or separation is close to the trailing-edge region within 10 percent of the chord length from the trailing edge.

For the NACA 0012 airfoil at zero sweep, all three programs predict C_L and C_D values that are in good agreement with experimental data as shown in figure 1(a). At higher angles of attack, the Dvorak and Woodward Program (DWP) underpredicted C_L while the GBP overpredicted C_L. When these C_L predictions trends are taken into account, DWP and GBP underestimate the drag coefficient at all angles of attack, whereas the Modified NASA Program (MNP) overestimated it. At 20° sweep, both DWP and GBP predict the same values for C_L, but relative to GBP, DWP predicts higher drag coefficients.

For the NACA 2424 airfoil in the unswept orientation, figure 2 shows that all three programs predicted linear C_L versus α curves. C_L values of DWP are in agreement with MNP and both of these predictions were consistently higher than those of GBP. The experimental C_L versus α curve is nonlinear primarily due to the higher thickness of the airfoil, but all these programs failed to predict this nonlinear thickness effect. In view of the C_L predictions, MNP overpredicted C_D; whereas DWP and GBP underestimated C_D. At 20° and 40° of sweep, DWP consistently predicted higher C_L and C_D values over GBP.

For the NACA 63-006 airfoil, figure 3 shows that for the unswept orientation, predictions of all programs are generally in good agreement with the experimental results. In the swept orientation, predictions of both DWP and GBP are in close agreement.

For the NACA 23012 airfoil, all three programs predicted (see fig. 4) linear C_L versus α curves for the unswept wing. DWP and MNP predictions of C_L are in good agreement with experimental data, while GBP predicted consistently higher values for C_L. The predictions of C_D by MNP are in good agreement with measurements. Figure 4(b) shows that DWP and GBP have underpredicted C_D, and the extent of disagreement with measurements can be seen to increase with increasing angle of attack. For the 20° swept case, C_L predictions by GBP are higher than those by DWP; whereas, DWP predicted higher values for C_D than did GBP. Further DWP predicted smaller stall angle. At 40° sweep, among the two programs DWP predicted higher values for both C_L and C_D.

The results for the TN D-7071 airfoil are shown in figure 5. The C_L and C_D predictions by all the three programs are in better agreement for this airfoil than for any of the other airfoils investigated in this report. Such good agreement is rather surprising considering the fact that this is an unusual airfoil designed for high lift. Departures in predictions occurred very close to the stall region. No conclusions can be drawn on C_D predictions because there are no experimental data available on C_D even for the 0° sweep case. At 20° sweep, the results are much like those at 0° sweep. At 40° sweep, GBP predicted early separation while DWP did not.

The results for the GA(W)-1 airfoil are shown in figure 6. At 0° sweep, predictions of C_L by DWP and MNP are in good agreement with experiment; whereas, GBP consistently underpredicted C_L. Although both DWP and GBP underpredicted C_D , the predictions are in good agreement with each other. MNP slightly underpredicted C_D. To eliminate the possible differences in results due to transition modeling, this airfoil was run at 0° sweep with fixed transition. The results are shown in figures 6(a) and 6(b). For each program, the trends predicted with free and fixed transition are similar and do not appear to be effected significantly by the transition modeling. At 20° and 30° sweeps, DWP predicted consistently higher values for C_L than did GBP. Both of these programs predict about the same values for C_D.

The DWP was run in all cases with the parameters for maximum number of iterations set at 6 and the value for convergence criterion on C_L set at 0.01. For the six airfoils tested, the convergence criterion was observed to be satisfied in under six iterations in most of the cases and only in a few cases the sixth iteration was computed. In all the cases where the sixth iteration was computed, C_L was observed to be within 0.015 of the previous iteration. The above comments are applicable only in the absence of catastrophic separation.

The GBP was run in all cases with the parameter for maximum number of iterations set at seven. C_L is observed to converge in all cases to a value within 0.01 of the previous iteration in the absence of catastrophic separation.

CONCLUSIONS

Six single-element airfoils are used as test cases to compare the performance of the three programs by Dvorak and Woodward (ref. 4), Gingrich and Bonner (ref. 5), and the modified NASA program (refs. 3 and 6). Based on the results obtained, the following conclusions can be drawn:

1. In the unswept orientation of the airfoils, all the three programs predicted the lift coefficient well for all the airfoils except for the 24-percent-thick airfoil. Further, the predicted C_L versus α curves are approximately linear for all the airfoils. In the swept orientation, the predictions of C_L by the two swept-wing programs are in good agreement for the NACA 0012, NACA 63-006, and TN D-7071 airfoils; whereas, for the NACA 2424 and GA(W)-1 airfoils, the Dvorak and Woodward program consistently predicted higher values for C_L.

2. For the airfoil designed for high lift, somewhat surprisingly all the programs predicted C_L accurately, and while there are no experimental data available to compare the drag coefficients with, the C_D predictions of all programs are in good agreement with each other.

3. In the unswept orientation, the drag coefficients are predicted satisfactorily at small angles of attack, and the predictions by the swept-wing programs progressively underestimated the drag coefficient as the stall region is approached. In general, the predictions of both C_L and C_D by the modified NASA program (which has no sweep capability) are in better agreement with measurements than the two swept-wing programs. For the airfoils in the swept orientation, as there are no published measurements, definitive conclusions cannot be drawn about the C_D predictions. At 20° sweep, Dvorak and Woodward program tended to predict higher C_D values than the Gingrich and Bonner program. However, at 40° sweep, there is little agreement between the predictions of the two programs.

4. The execution times are approximately the same for all the three programs. In general, the time increased with increasing sweep angles. For an angle-of-attack case, the typical execution times on the CDC 6600 computer are 20, 25, and 30 seconds, respectively, corresponding to the 0°, 20°, and 40° sweep angles. For a given case, the execution times of the programs are typically within 5 seconds of each other. The memory required for the Dvorak and Woodward program is approximately 150K octal words and that for the Gingrich and Bonner program is approximately 65K. The former is higher primarily because of the multi-element capability of that program.

REFERENCES

1. Langan, T. J.; and Wang, H. T.: Evaluation of Lifting-Surface Programs for Computing the Pressure Distribution on Planar Foils in Steady Motion. Naval Ship Research and Development Center Rep. 4021, May 1973

2. Stevens, W. A.; Goradia, S. H.; and Braden, J. A.: Mathematical Model for Two-Dimensional Multi-Component Airfoils in Viscous Flow. NASA CR-1843, 1971

3. Smetana, Frederick O.; Summary, Delbert C.; Smith, Neill S.; and Carden, Ronald K.: Light Aircraft Lift, Drag, and Moment Prediction - A Review and Analysis. NASA CR 2523, 1975

4. Dvorak, F. A.; and Woodward, F. A.: A Viscous/Potential Flow Interaction Analysis Method for Multi-Element Infinite Swept Wings. NASA CR-2476, 1974

5. Gingrich, P.; and Bonner, E.: Prediction of Infinite Wing Viscous Characteristics at Subcritical Speeds. NA-74-758, Rockwell-International, December 1974

6. Morgan, Harry L., Jr.: A Computer Program for the Analysis of Multi-Element Airfoils in Two-Dimensional Subsonic, Viscous Flow. NASA SP-347, pt. II, 1975, pp. 713-747

7. Labrujere, Th. E.; Loeze, W.; and Slooff, W.: An Approximate Method for the Determination of the Pressure Distribution on Wings in the Lower Critical Speed Range. AGARD CP 35, article no. 17, 1968

8. Spence, D. A.: Prediction of the Characteristics of Two-Dimensional Airfoils. J. Aeronauti. Sci., vol. 21, no. 9, Sept. 1954

9. Cumpsty, N. A.; and Head, M. R.: The Calculation of Three-Dimensional Turbulent Boundary Layers, Part II: Attachment - Line Flow on an Infinite Swept Wing. Aeronaut. Quart., vol. XVIII, May 1967, pp. 150-164

10. Smith, P. D.; and Young, A. D.: Approximate Solutions of the Three-Dimensional Laminar Boundary Layer Momentum Integral Equations. CP 1064, Brit. A.R.C., 1969

11. Granville, P. S.: The Calculation of the Viscous Drag of Bodies of Revolution. David Taylor Model Basic Rep. 249, 1953

12. Schlichting, H.; and Ulrich, A.: Zur Berechnung des Umschlages Laminar-Turbulent (On the Calculation of Laminar-Turbulent Transition). Jahrbuch 1942 der Deutchen Luftfahrt-Forschung, pp. 8-35

13. Smith, A. M. O.: Transition Pressure Gradient and Stability Theory. Proc. 9th Internat. Cong. Appl. Mech., Brussels, vol. 4, 1957, pp. 234-244

14. Schlichting, H. (J. Krestin, transl.): Boundary Layer Theory. Third ed., McGraw-Hill Book Co., Inc., 1960

15. Brown, W. B.: A Stability Criterion for Three-Dimensional Laminar Boundary Layers. Boundary Layer and Flow Control, vo. 2, (Lachman, G. V.,ed.), Pergamon Press, 1961

16. Cumpsty, N. A.; and Head, M. R.: The Calculation of Three-Dimensional Turbulent Boundary Layers, Part I: Flow Over the Rear of an Infinite Swept Wing. Aeronaut. Quart, vol. XVIII, Feb. 1967, pp. 55-84

17. Mager, H.: Generalization of Boundary Layer Momentum Integral Equations to Three-Dimensional Flows Including Those of Rotating Systems. NACA TR 1067, 1952

18. Smith, P. D.: An Integral Prediction Method for Three-Dimensional Compressible Turbulent Boundary Layers. R&M 3739, Brit. A.R.C., 1974

19. Squire, H. B.; and Young, A. D.: The Calculation of the Profile Drag of Airfoils. R&M 1838, Brit. A.R.C., 1938

20. Cumpsty, N. A.; and Head, M. R.: The Calculation of the Three-Dimensional Boundary Layer, Part III: Comparison of Attachment Line Calculations with Experiment. Aeronaut. Quart., vol. 20, May 1969, pp. 99-113

21. Abbott, Ira H.; and von Doenhoff, A. E.: Theory of Wing Sections. Dover Publications, Inc., New York, 1959

22. McGhee, R. J.; and Beasley, W. D.: Low-Speed Aerodynamic Characteristics of a 17-Percent-Thick Airfoil Section Designed for General Aviation Applications. NASA TN D-7428, 1973

23. van den Berg, B.; Elsenaar, A.; and Lindhout, J. P. F.: Measurements in an Incompressible Three-Dimensional Turbulent Boundary Layer, Under Infinite Swept-Wing Conditions, and Comparison with Theory. J. Fluid Mech., vol. 70, pt. 1, 1975, pp. 127-148

24. Bingham, Gene J.; and Chen, Allen Wen-Shin: Low-Speed Aerodynamic Characteristics of an Airfoil Optimized for Maximum Lift Coefficient. NASA TN D-7071, 1972

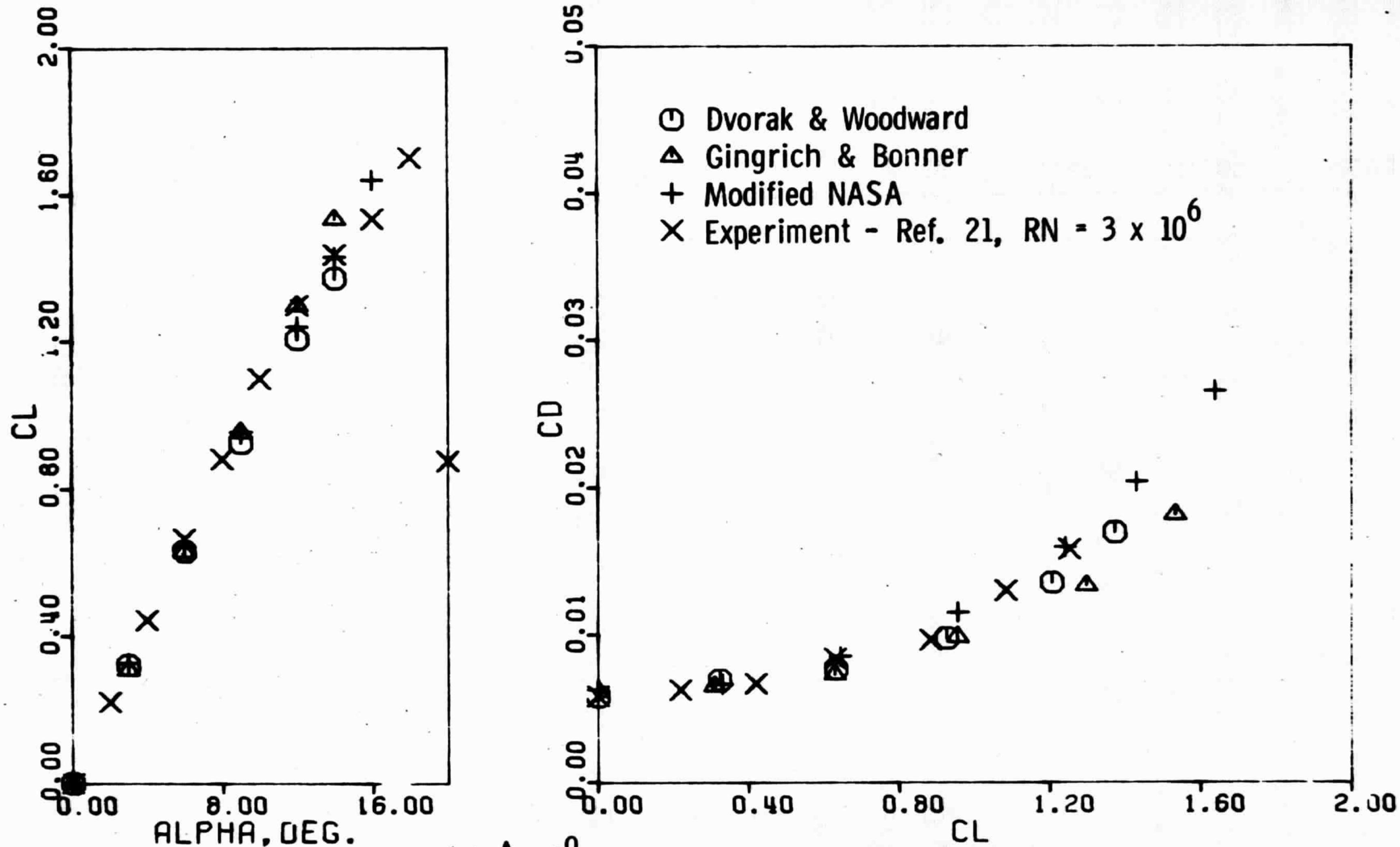

(a) $\Lambda = 0^0$

Figure 1. - Comparison of predicted lift and drag coefficients of NACA-0012 airfoil at RN = 3.335 x 10^6, M = 0.14, and with free transition.

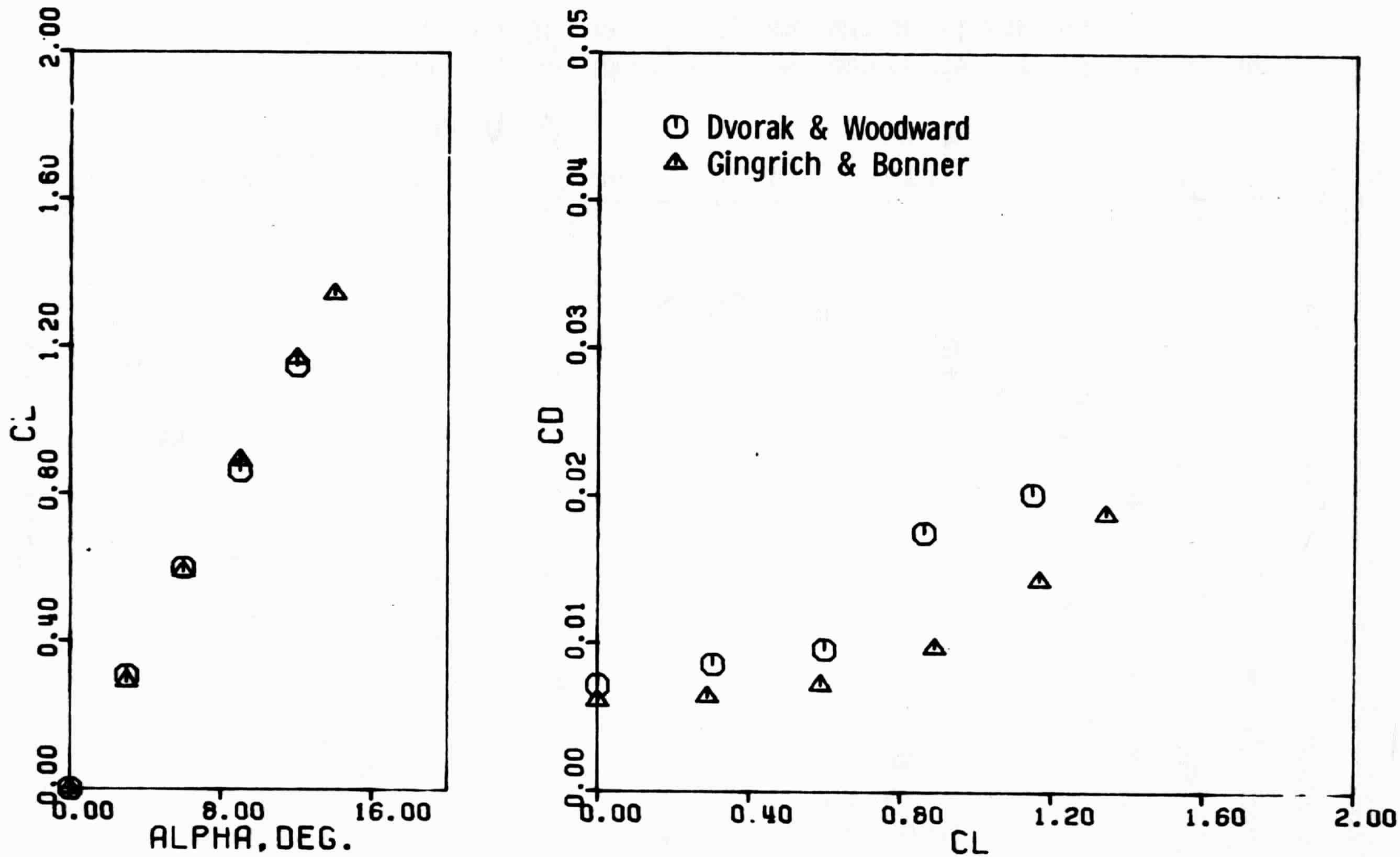

(b) $\Lambda = 20^0$

Figure 1. - Continued.

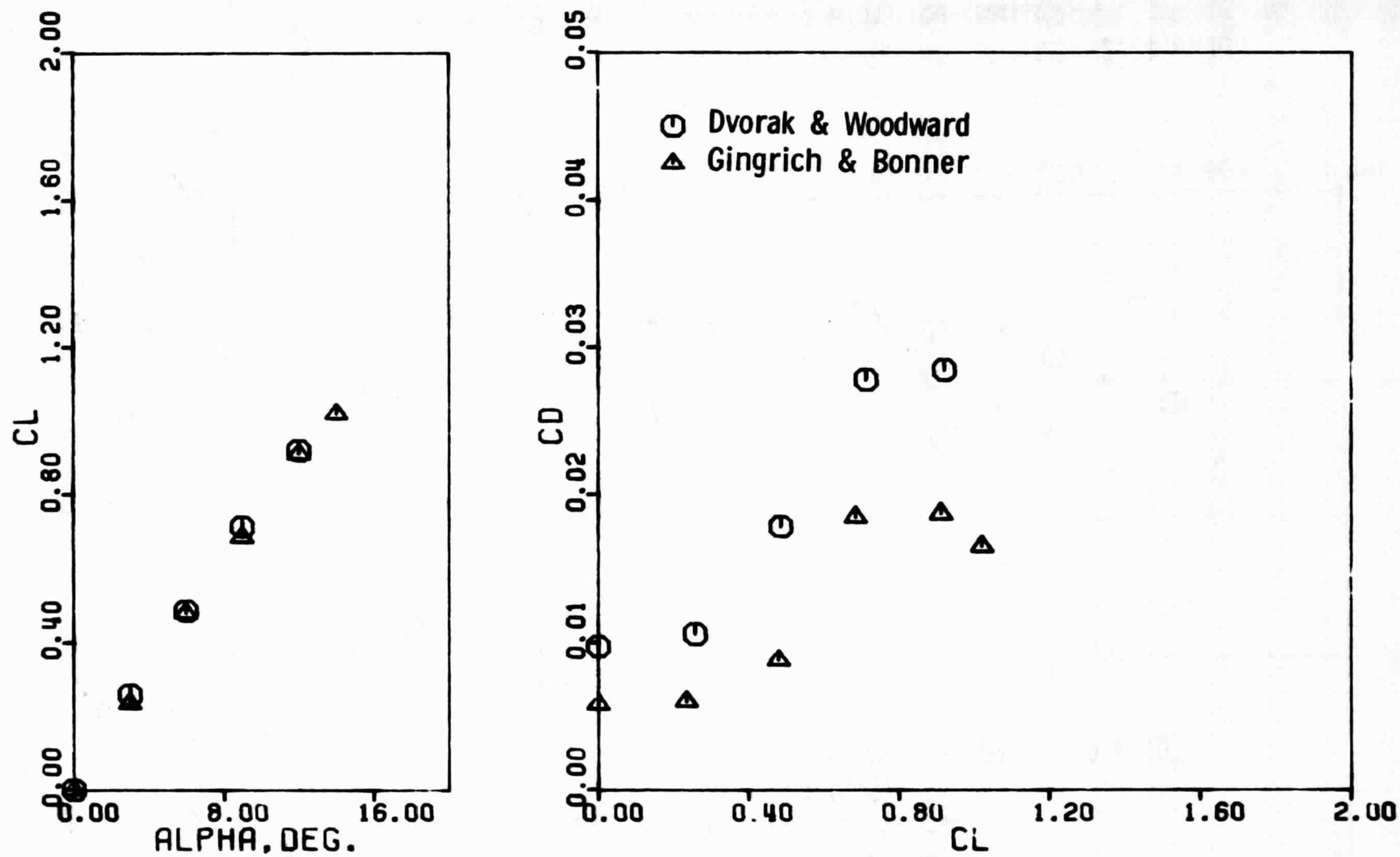

(c) $\Lambda = 40^0$

Figure 1. - Concluded

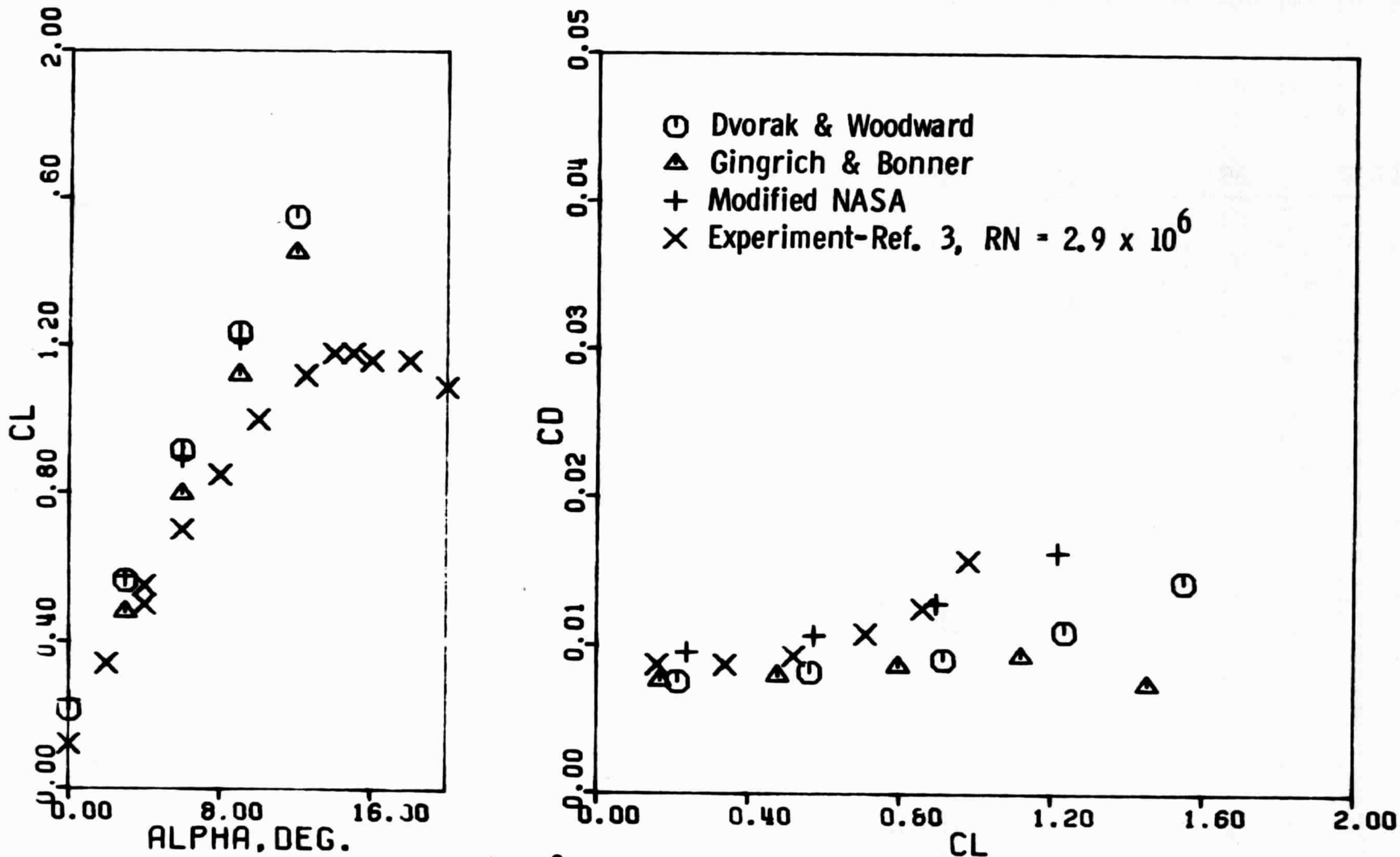

(a) $\Lambda = 0^0$

Figure 2. - Comparison of predicted lift and drag coefficients of NACA-2424 airfoil at RN = 3.335×10^6, M = 0.14, and with free transition.

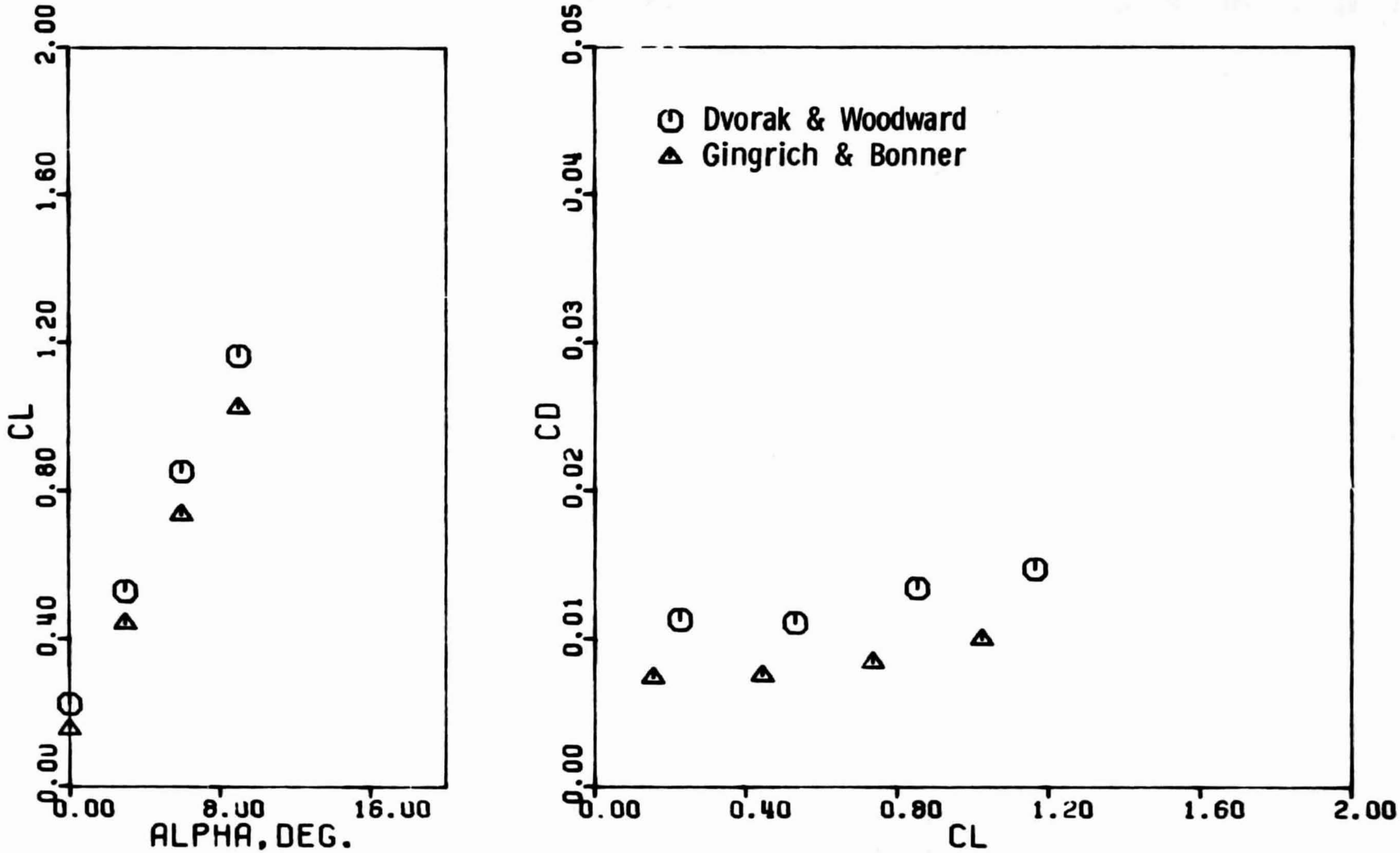

(b) $\Lambda = 20^0$

Figure 2. - Continued

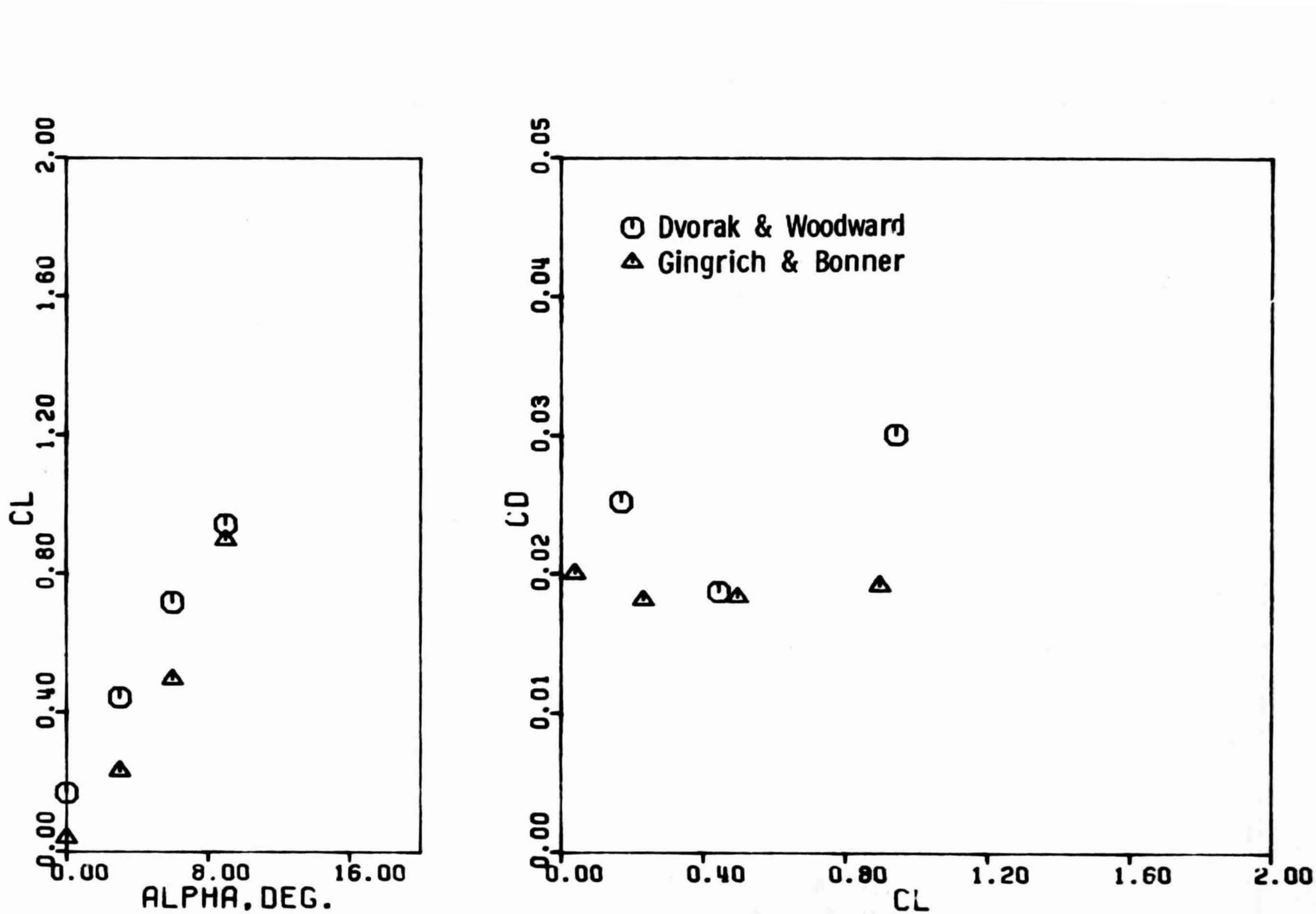

(c) $\Lambda = 40^0$

Figure 2. - Concluded.

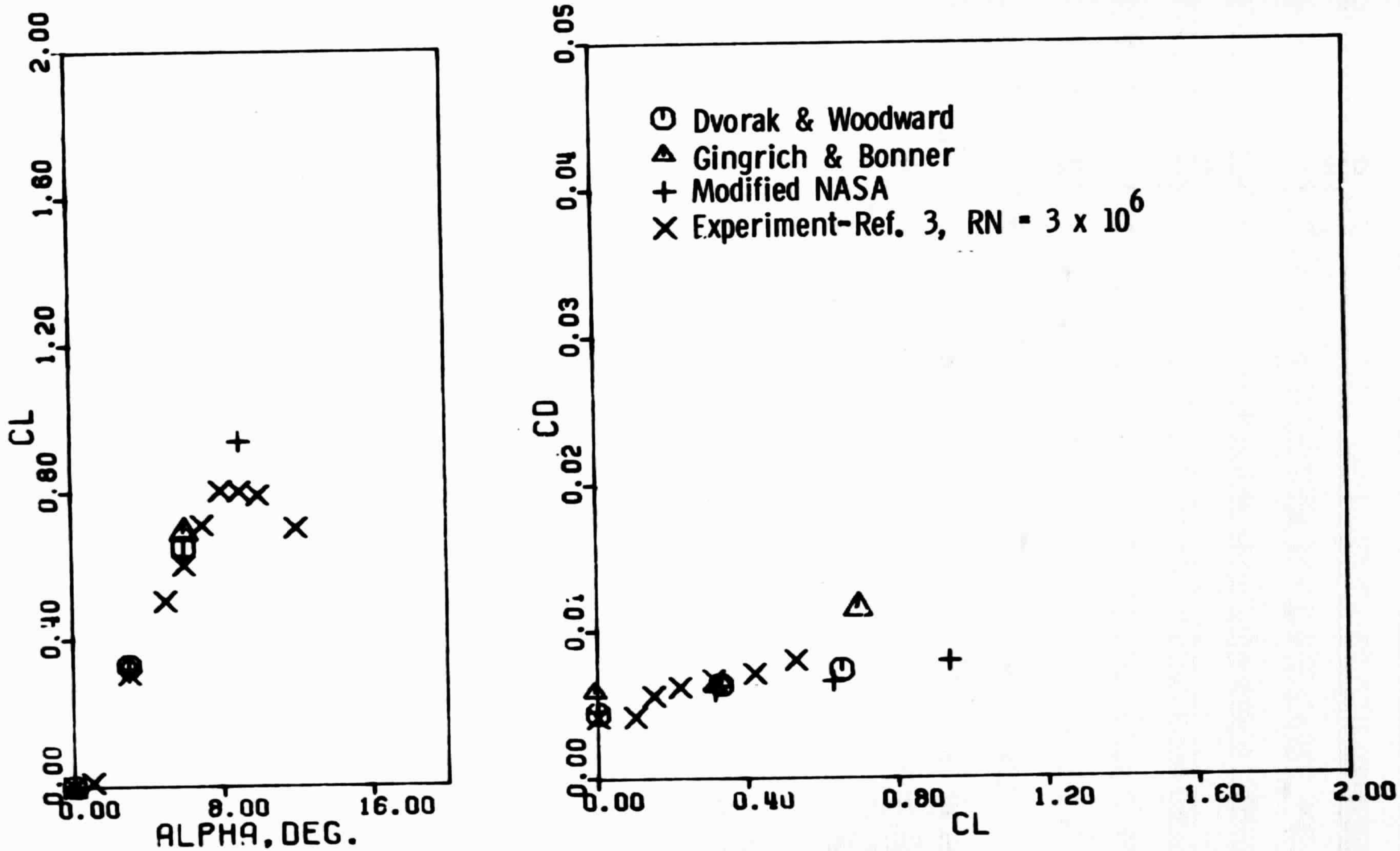

(a) $\Lambda = 0^0$

Figure 3. - Comparison of predicted lift and drag ocefficients of NACA 63-006 airfoil at RN = 3.335×10^6, M = 0.14, and with free transition.

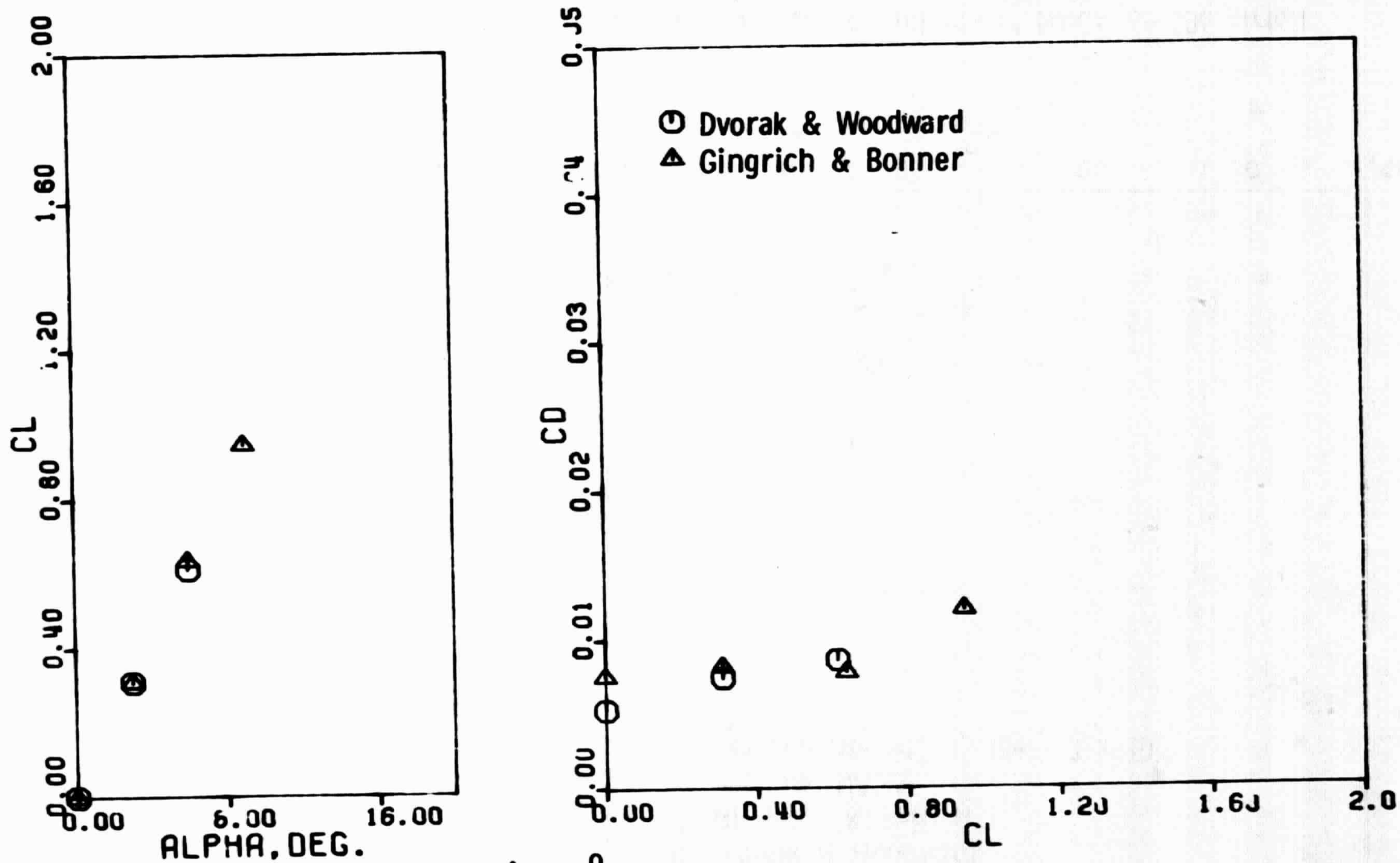

(b) $\Lambda = 20^0$

Figure 3. - Continued.

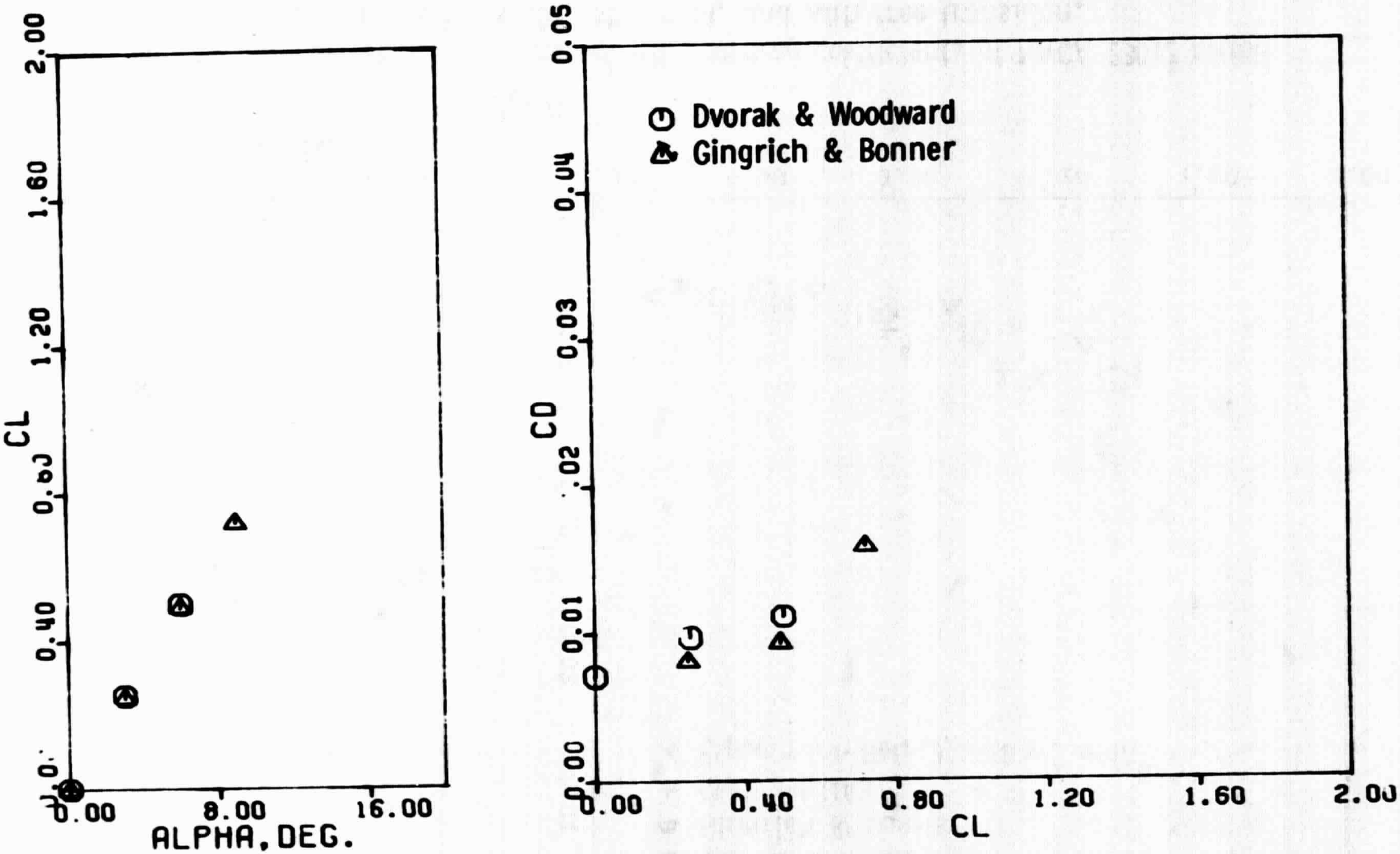

(c) $\Lambda = 40^0$

Figure 3. - Concluded

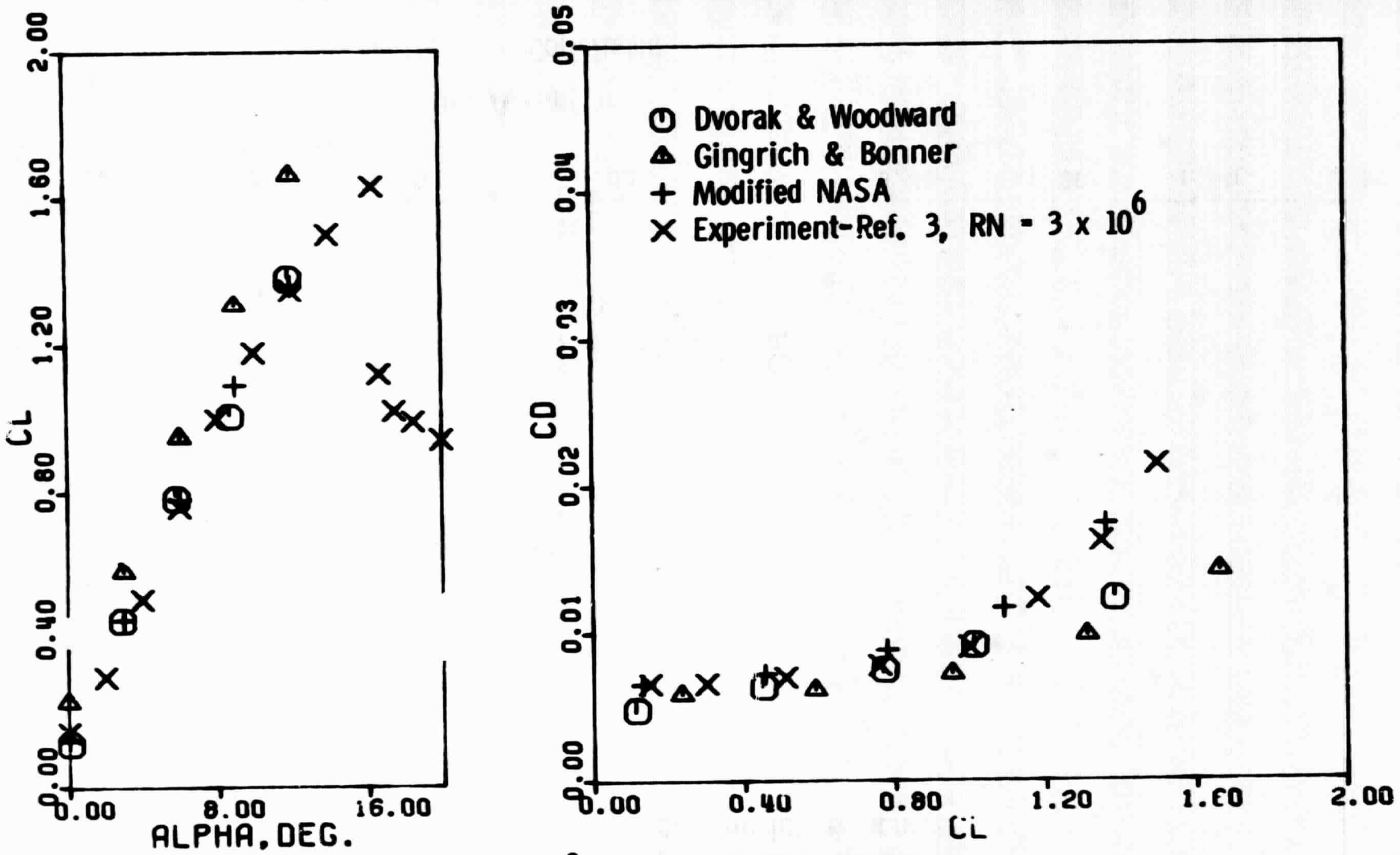

(a) $\Lambda = 0^0$

Figure 4. - Comparison of predicted lift and drag coefficients of NACA 23012 airfoil at RN = 3.335×10^6, M = 14, and with free transition.

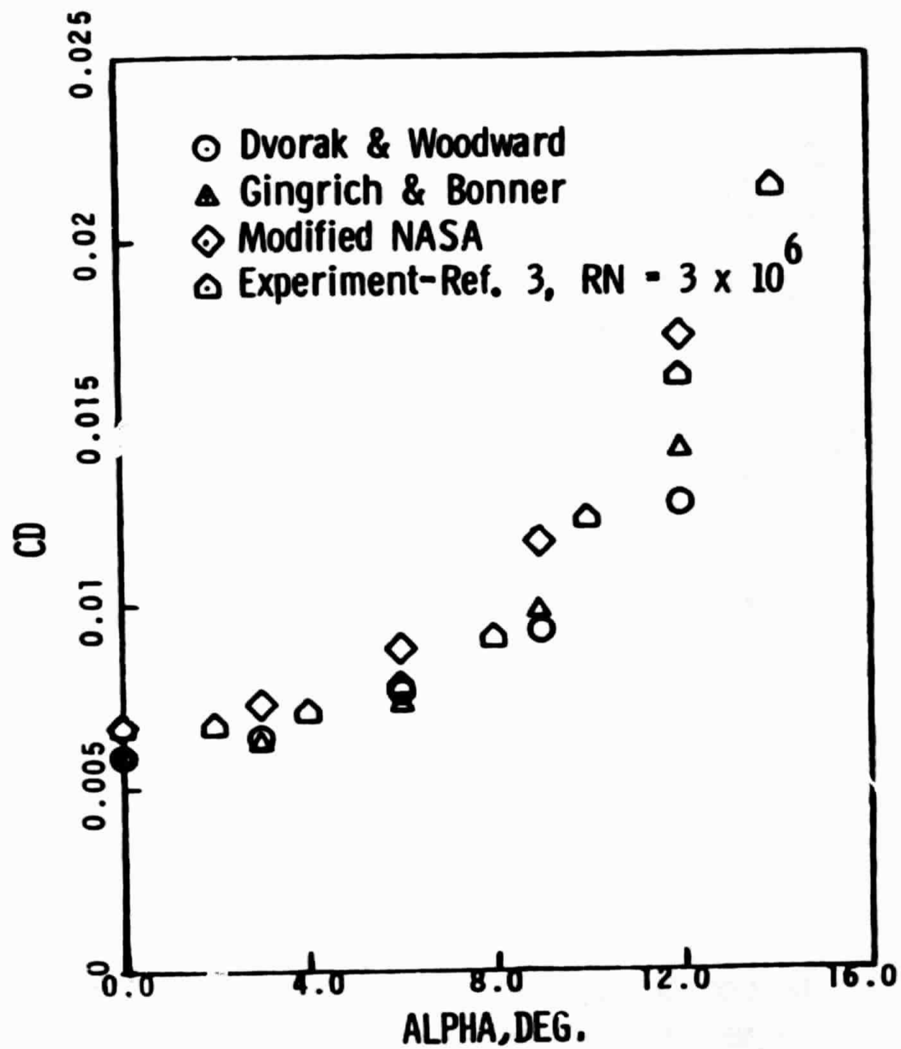

(b) $\Lambda = 0^0$

Figure 4. - Continued.

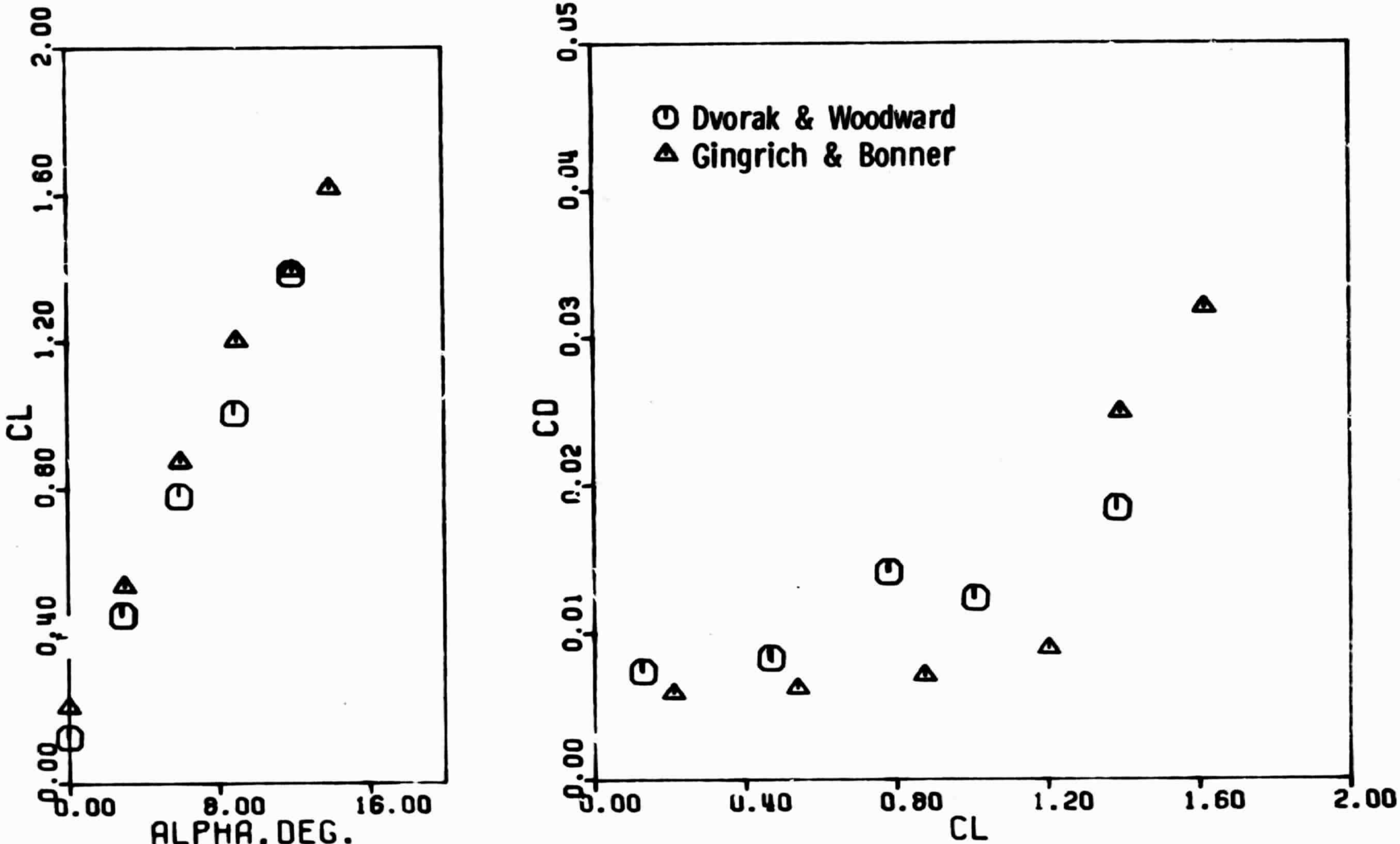

(c) $\Lambda = 20^0$

Figure 4. - Continued.

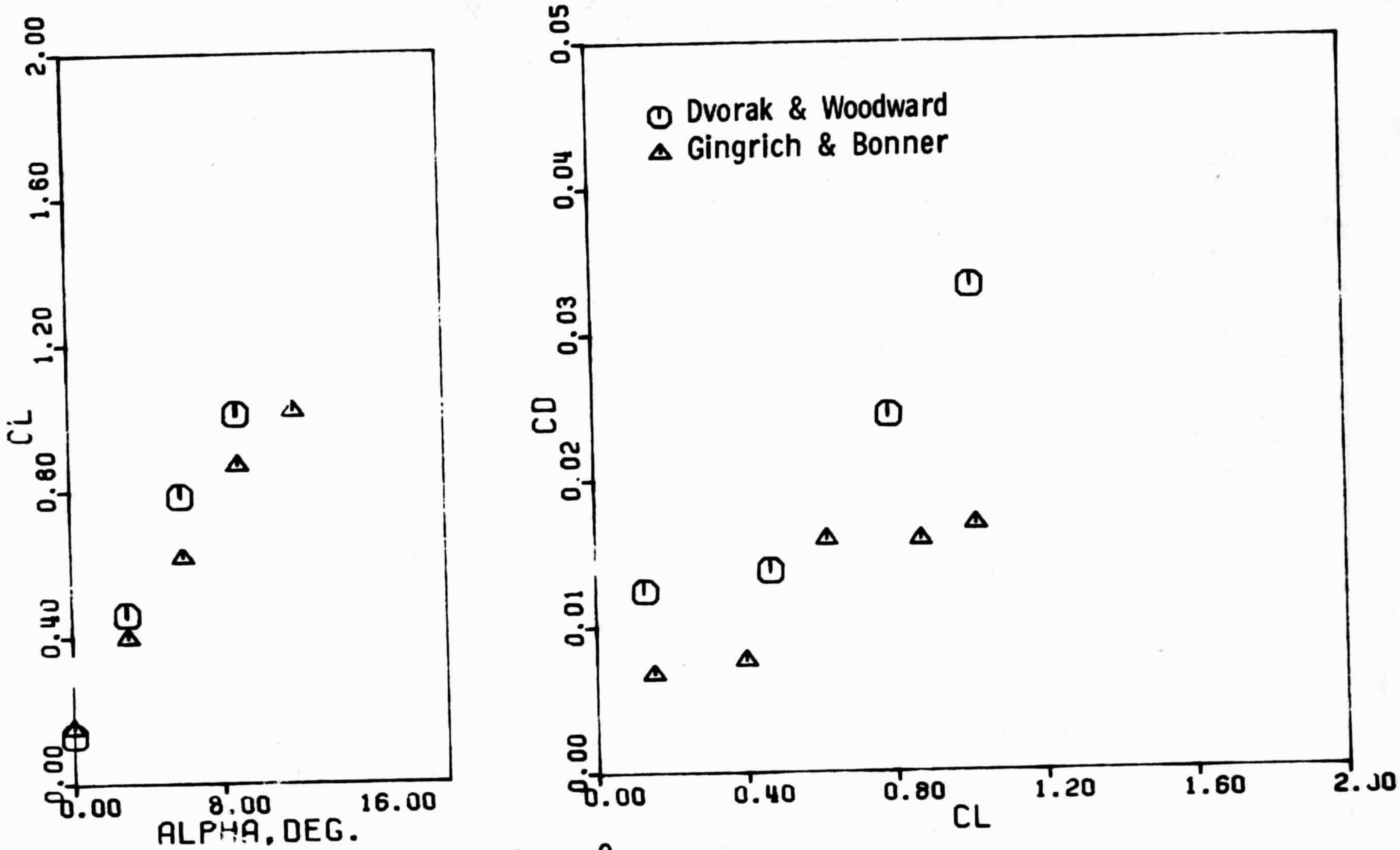

(d) $\Lambda = 40^0$

Figure 4. - Concluded

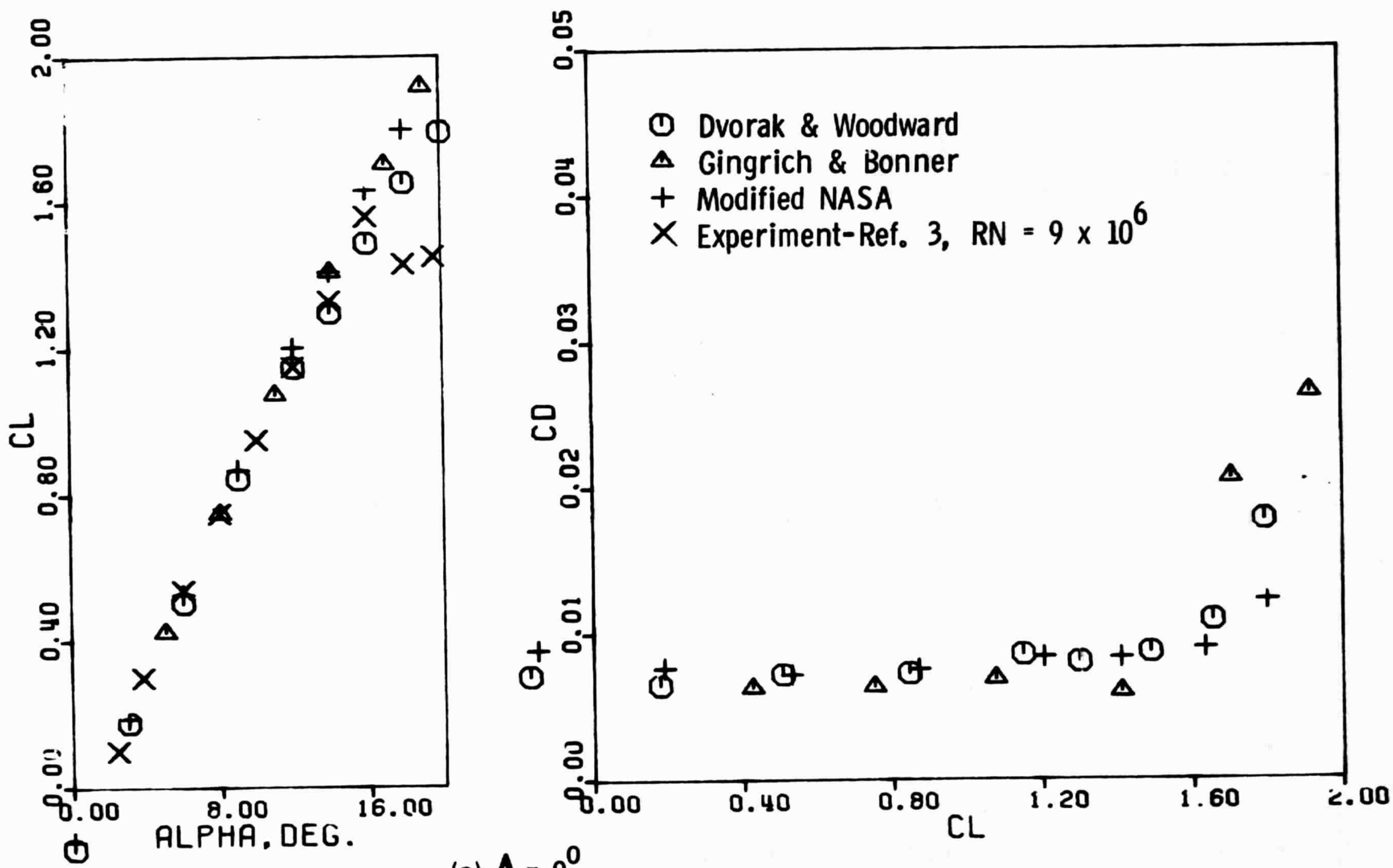

(a) $\Lambda = 0^0$

Figure 5. - Comparison of predicted lift and drag coefficients of TN D-7071 airfoil at RN = 9.06×10^6, M = 0.14, and with free transition.

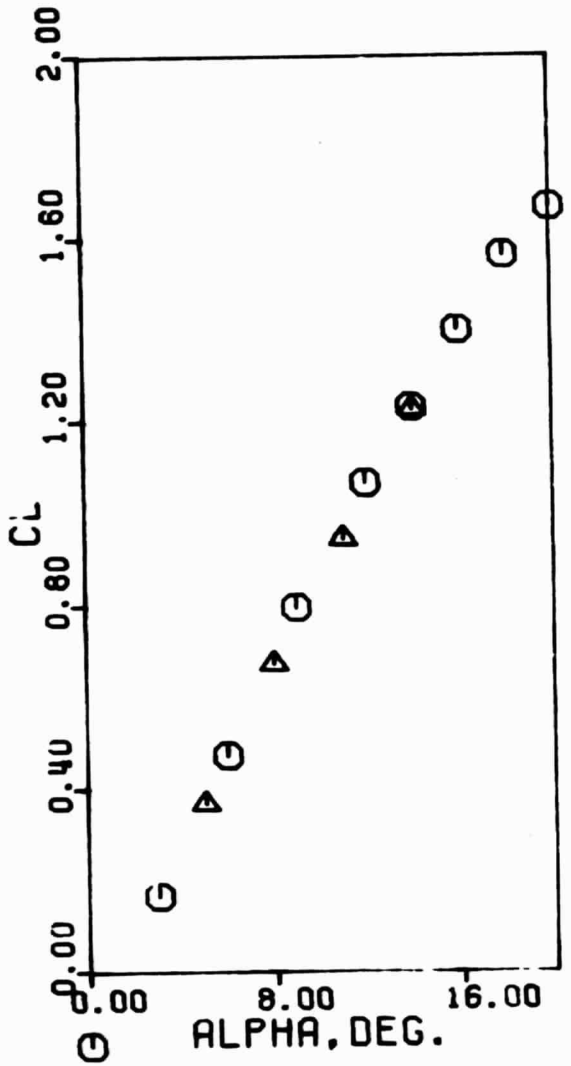

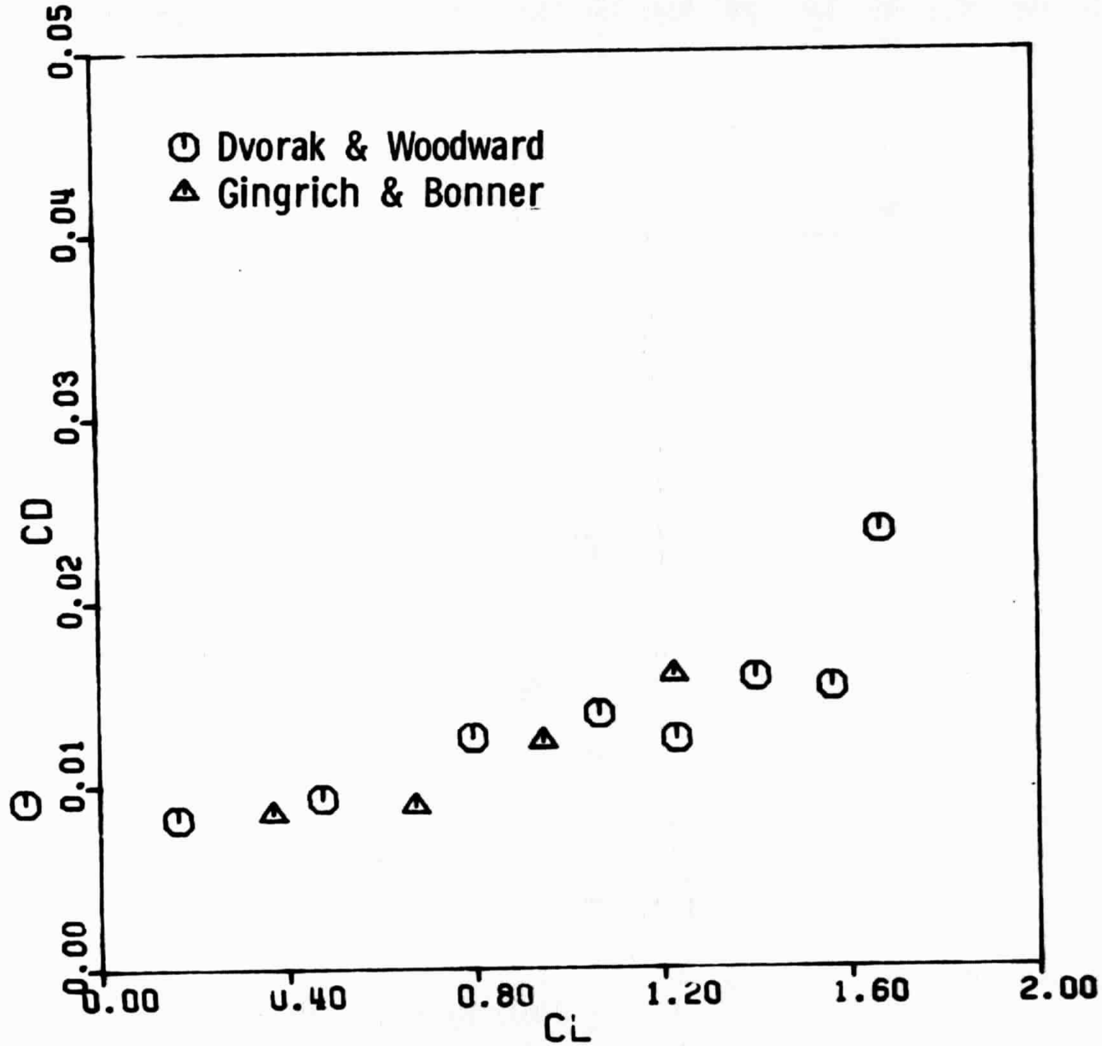

(b) $\Lambda = 20^0$

Figure 5. - Continued.

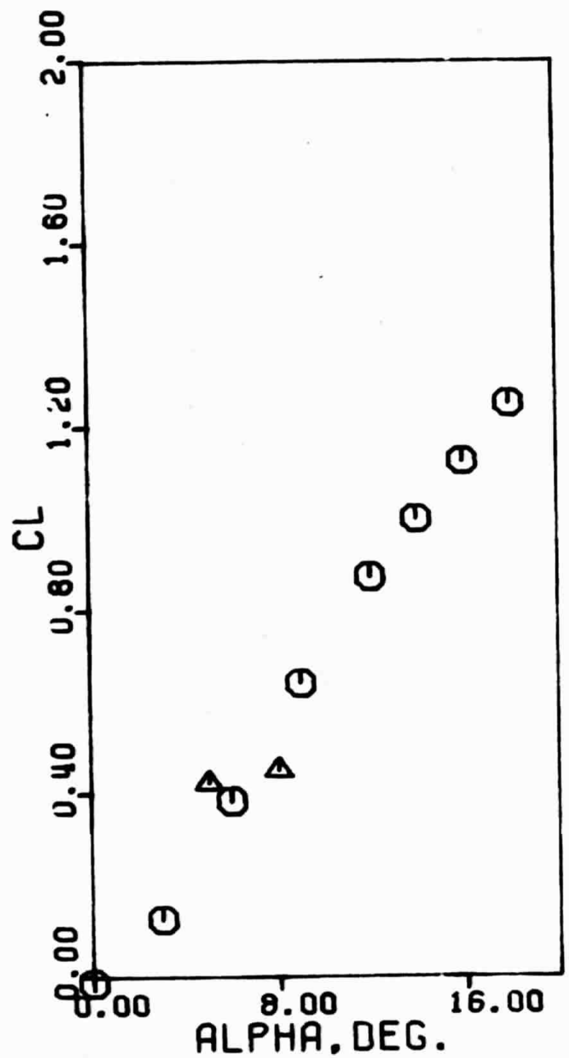

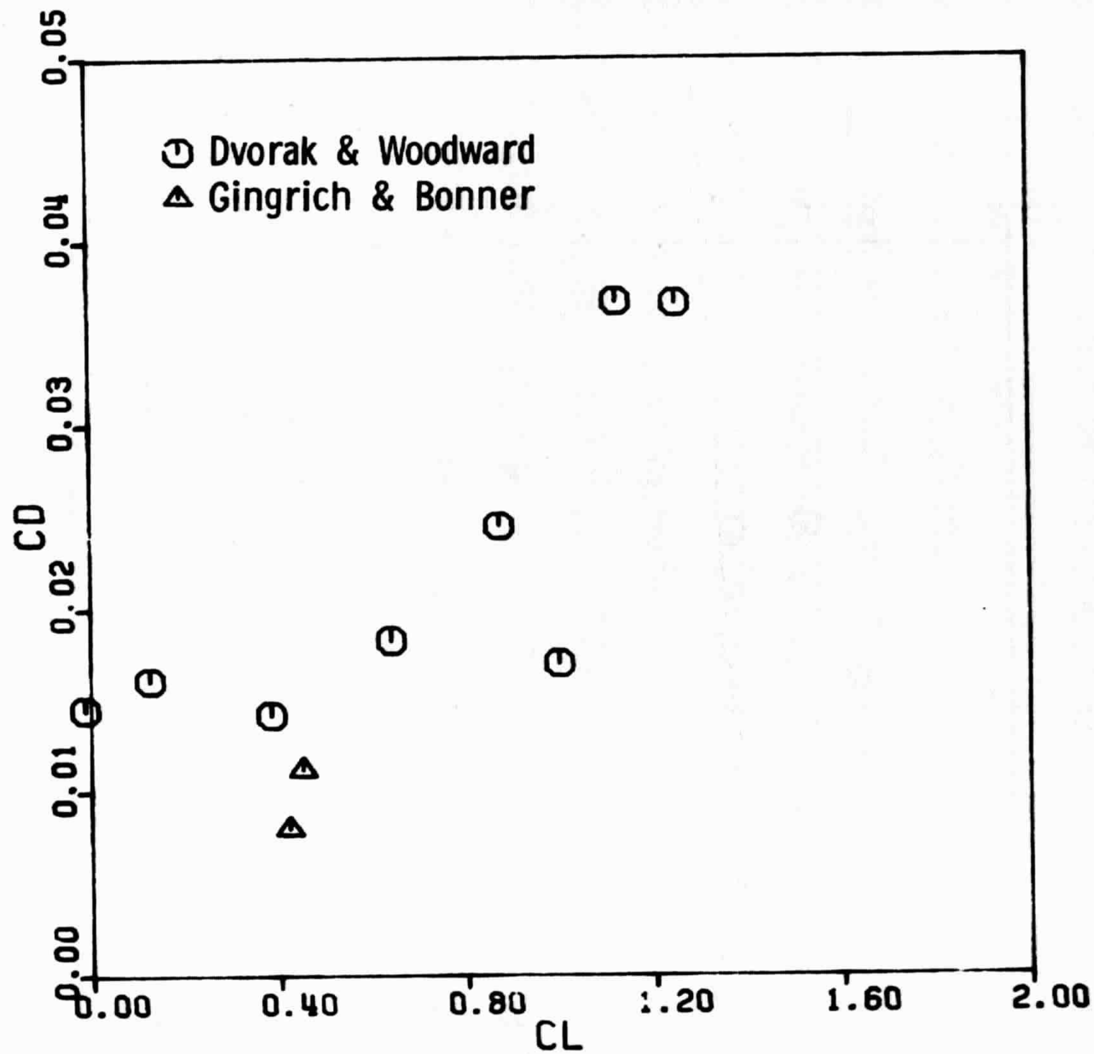

(c) $\Lambda = 40^0$

Figure 5. - Concluded

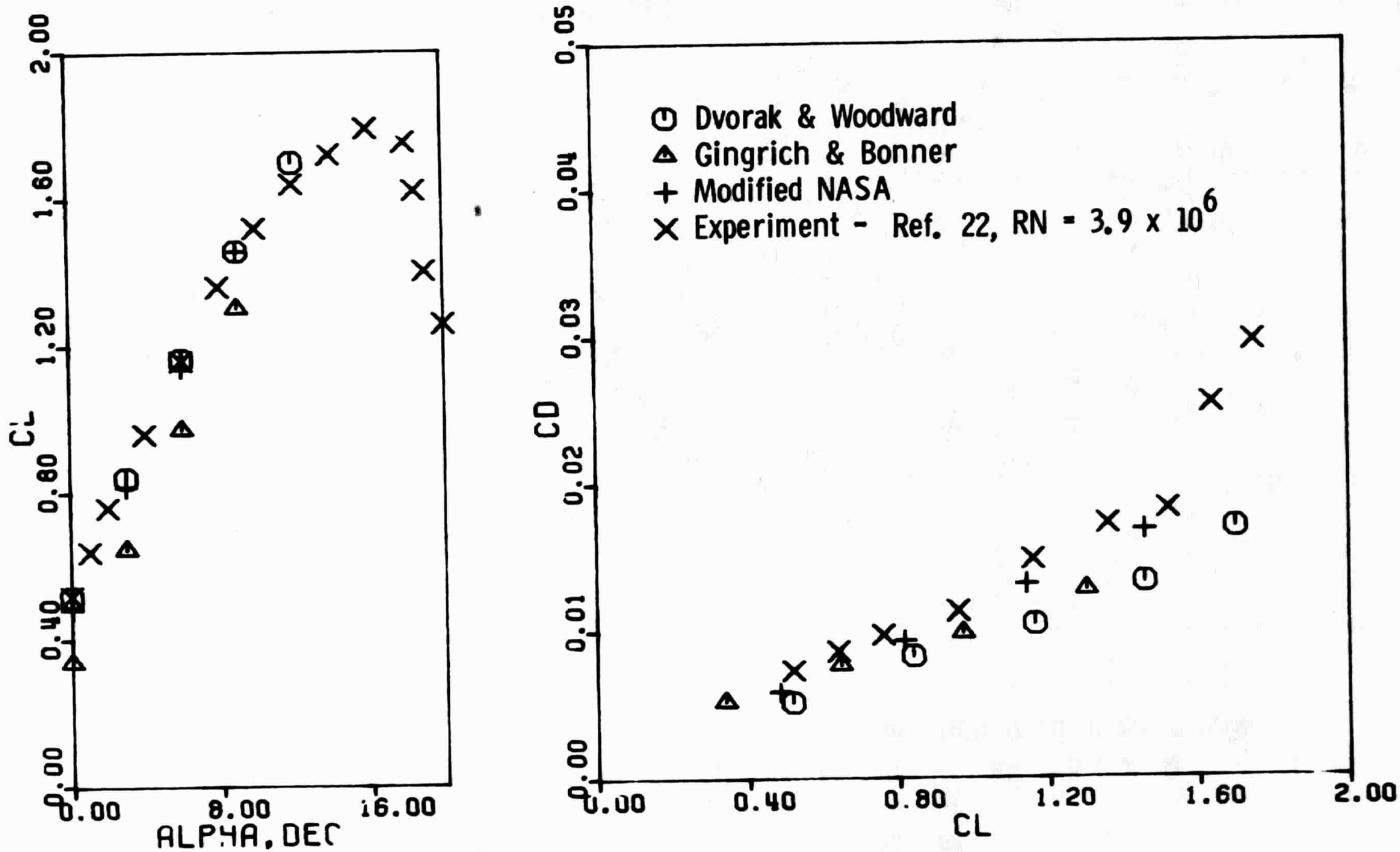

(a) $\Lambda = 0^0$, free transition

Figure 6. - Comparison of predicted lift and drag coefficients of GA(W)-1 airfoil at RN = 3.335×10^6, M = 0.14.

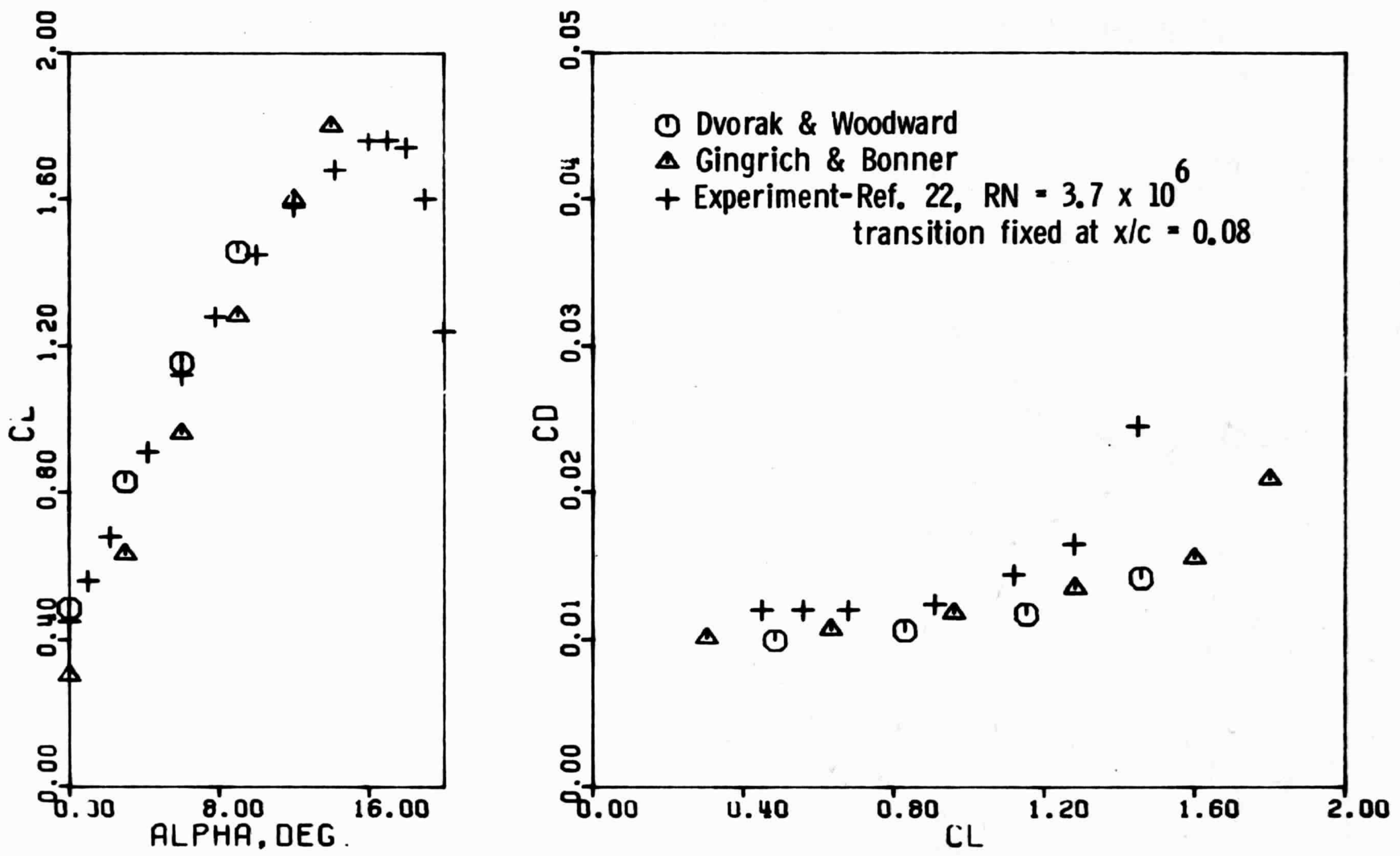

(b) $\Lambda = 0^{\circ}$, Transition fixed at x/c = 0.075

Figure 6. - Continued.

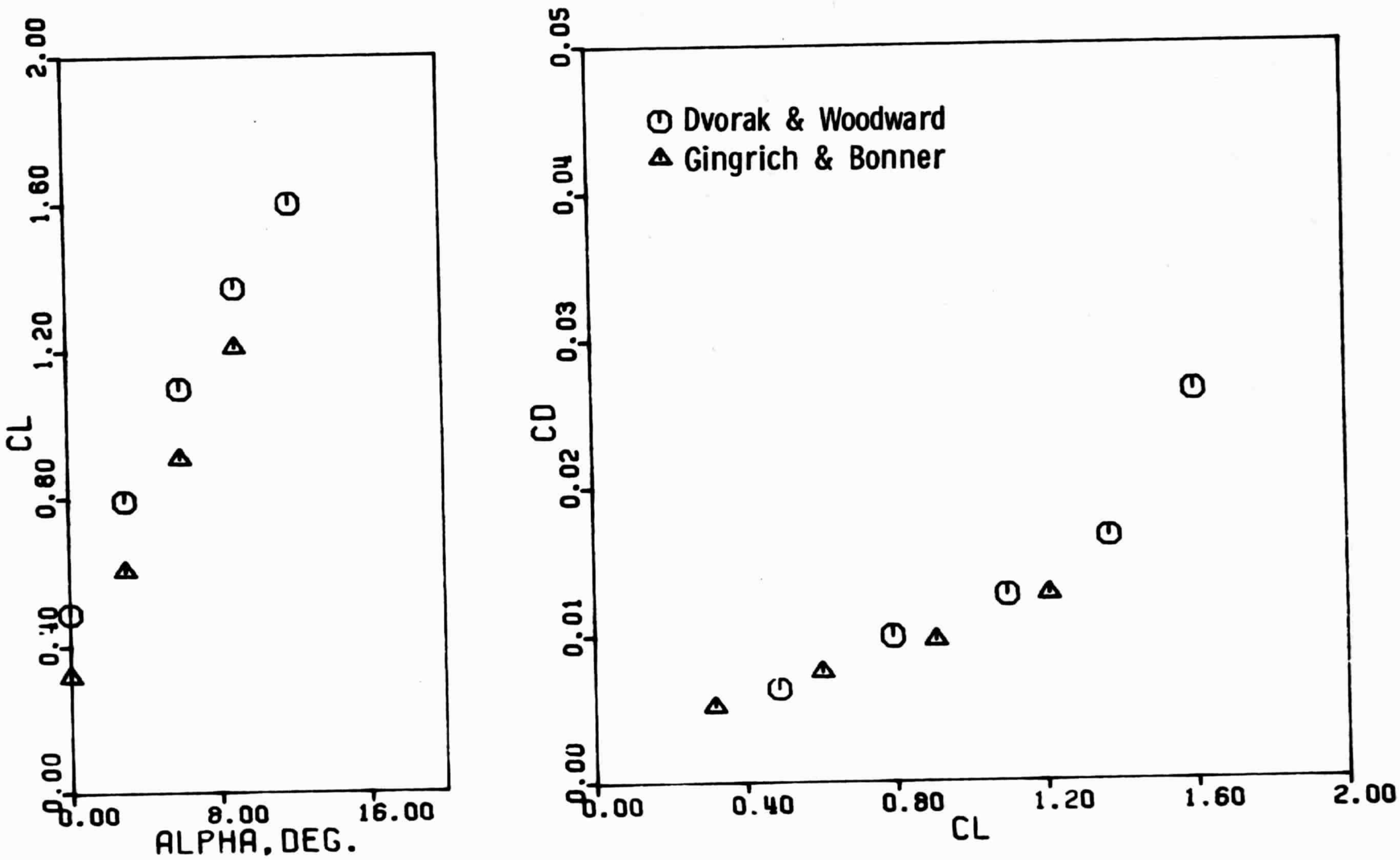

(c) $\Lambda = 20^0$, free transition

Figure 6. - Continued.

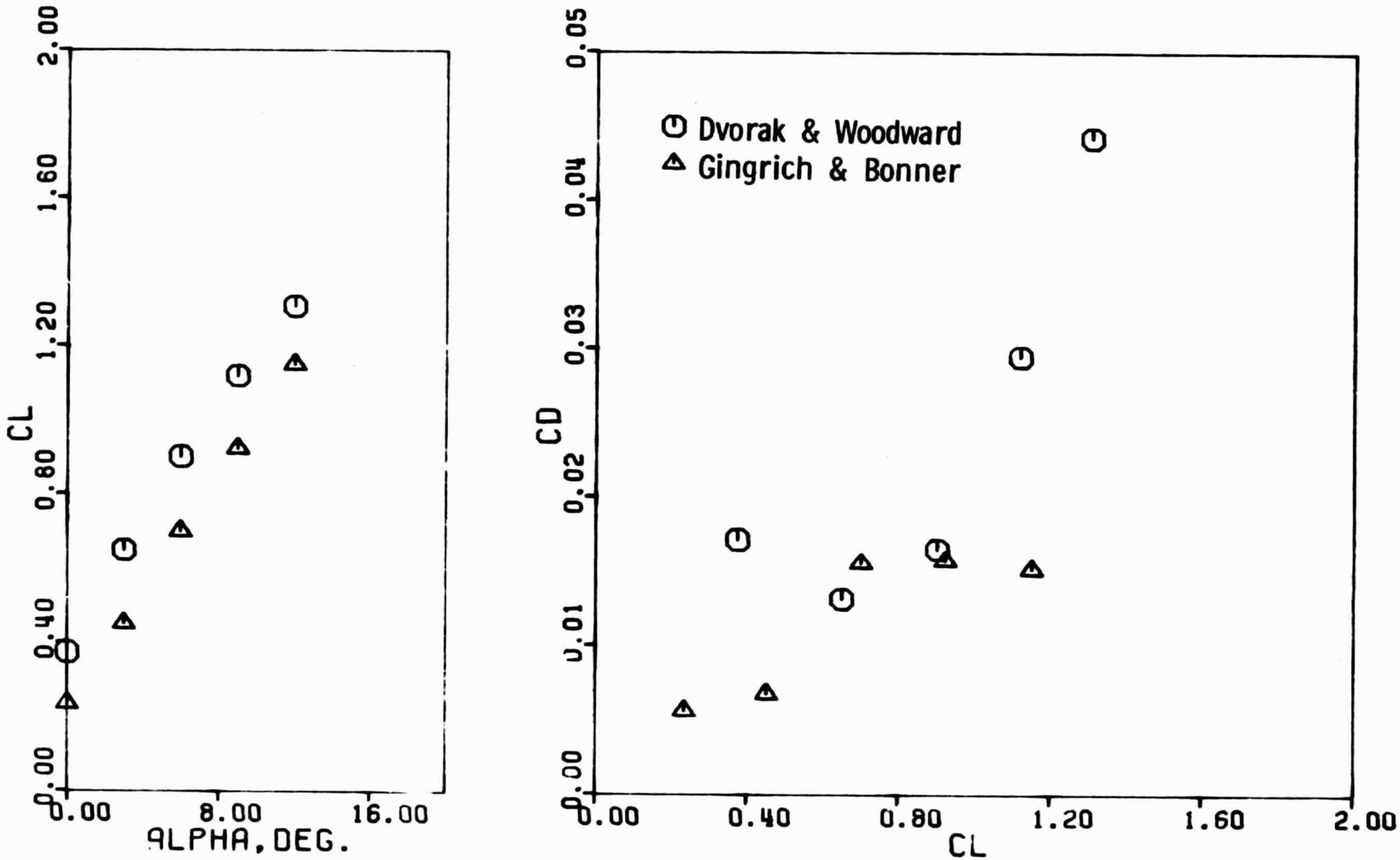

(d) $\Lambda = 40^0$, free transition

Figure 6. - Concluded.